A hormone complex of FABP4 and nucleoside kinases regulates islet function

Kacey J. Prentice[1], **Jani Saksi**[1], **Lauren T. Robertson**[1], **Grace Y. Lee**[1], **Karen E. Inouye**[1], **Kosei Eguchi**[1], **Alexandra Lee**[1], **Ozgur Cakici**[1], **Emily Otterbeck**[1], **Paulina Cedillo**[1], **Peter Achenbach**[2], **Anette-Gabriele Ziegler**[2], **Ediz S. Calay**[1], **Feyza Engin**[1,3], **Gökhan S. Hotamisligil**[1,4,*]

[1]Sabri Ülker Center for Metabolic Research, Harvard T.H. Chan School of Public Health, Department of Molecular Metabolism; Boston, MA, USA

[2]Institute of Diabetes Research, Helmholtz Zentrum Munchen, German Research Center for Environmental Health, Munich-Neuherberg, Germany

[3]Departments of Biomolecular Chemistry and Medicine, Division of Endocrinology, Diabetes and Metabolism, University of Wisconsin-Madison School of Medicine and Public Health, Madison, WI, USA

[4]Broad Institute of Harvard and MIT, Cambridge, MA, USA.

Summary

Liberation of energy stores from adipocytes is critical to support survival in times of energy deficit, however, uncontrolled or chronic lipolysis associated with insulin resistance and/or insulin insufficiency, disrupts metabolic homeostasis[1,2]. Coupled to lipolysis is the release of a recently identified hormone, fatty acid-binding protein 4 (FABP4)[3]. While circulating FABP4 levels have been strongly associated with cardiometabolic diseases in both preclinical models and humans[4–7], no mechanism of action has yet been described[8–10]. Here, we show that hormonal FABP4 forms a novel functional hormone complex with Adenosine Kinase (ADK) and Nucleoside Diphosphate Kinase (NDPK) to regulate extracellular ATP and ADP levels. We identify a substantial impact of this hormone on beta-cells and given the central role of beta-cell function in both the control of lipolysis and development of diabetes, postulate that hormonal FABP4 is a key regulator of an adipose-beta-cell endocrine axis. Antibody-mediated targeting of this hormone complex improves

metabolic outcomes, enhances beta-cell function, and preserves beta-cell integrity to prevent both type 1 and type 2 diabetes. Thus, the FABP4-ADK-NDPK complex, Fabtin, represents a previously unknown hormone and mechanism of action integrating energy status with the function of metabolic organs, representing a promising target against metabolic disease.

FABP4 targeting enhances beta-cell mass

This project was inspired by the observation of an increase in islet number by gross examination of the pancreata of lean FABP4$^{-/-}$ mice *in vivo* (Figure 1a), with the presence of islets being confirmed by dithizone staining (Figure S1a). Detailed analysis revealed that lean FABP4$^{-/-}$ mice exhibited significantly higher beta-cell mass and pancreatic insulin content compared to wild type (WT) littermates (Figure 1b–d). There was not a general increase in endocrine cells, as there was no difference in glucagon positive area (Figure S1b,c). Functionally, islets isolated from FABP4$^{-/-}$ mice demonstrated significantly increased glucose-stimulated insulin secretion (GSIS) (Figure 1e). Importantly, FABP4 is not expressed in islet endocrine cells or the clonal beta-cell line INS1 (Figure S1d,e). Thus, this cell type provides an opportunity to examine the specific role of hormonal FABP4 and the mechanisms underlying its actions.

To further support the paracrine/endocrine role of FABP4 *in vivo*, we used a monoclonal antibody (CA33, herein active antibody/a-Ab), the efficacy of which was determined in diet-induced obesity (DIO) as improving metabolic parameters[11]. Treatment of WT DIO mice with a-Ab for three weeks reduced 6hr fasting glucose levels and improved glycemic excursion during glucose tolerance test (GTT) (Figure 1f,g). Examination of a-Ab-treated DIO mice pancreata revealed increased islet number, consistent with lean FABP4$^{-/-}$ mice, and a trend toward increased beta-cell mass (Figure 1h–j). Thus, hormonal FABP4 influences beta-cell mass *in vivo*.

Hormonal FABP4 is elevated in T1D

It is well-established that FABP4 is elevated in T2D[4] and correlates with BMI. We investigated if hormonal FABP4 is also regulated in T1D, independent of adiposity and insulin resistance, contributing to beta-cell dysfunction directly. We evaluated serum from normoglycemic (NGT) individuals with or without autoantibody positivity and new-onset T1D patients (<1 year) from the BABYDIAB and DIMELLI cohorts[12–14]. Serum FABP4 was significantly elevated (~1.6-fold) in new-onset T1D individuals compared to both NGT groups (Figure 1k; Table S1). In a second population (BRI Cohort) of older T1D patients with various duration of disease, serum FABP4 levels significantly correlated with HbA1c (r^2=0.16, p=0.005), suggesting FABP4 is associated with glycemic control (Figure 1l; Table S2,S3). To complement these analyses, we quantified serum FABP4 from WT female non-obese diabetic (NOD) mice, comparing levels one week before T1D onset and at the time of diagnosis to age-matched non-diabetic controls. FABP4 was significantly increased both shortly before and in new-onset T1D mice (Figure 1m). Thus, circulating FABP4 levels are regulated before and immediately after impairment of glycemic control, suggesting that

hormonal FABP4 may have a role in beta-cell failure and pathogenesis of both T1D and T2D.

To explore the effect of antibody targeting of secreted FABP4 in T1D, we utilized WT female NOD mice matched for age, weight, blood glucose, plasma insulin, and circulating FABP4 (Figure S1f–i). Mice were treated twice weekly with a-Ab, PBS, or a control antibody of the same isotype (c-Ab) starting at 10 weeks of age, when insulitis had already been established. A-Ab significantly protected against development of T1D (Figure 1n). Among diabetic mice, a-Ab-treated animals had significantly reduced blood glucose and higher plasma insulin levels, suggesting a less severe diabetes phenotype (Figure 1o,p). This protection is similarly observed in FABP4$^{-/-}$ NOD mice[15]. Throughout the study there were no differences in blood glucose, body weight, or plasma insulin levels among non-diabetic mice (Figure S1j–l). Consistent with FABP4$^{-/-}$ and a-Ab treated DIO mice, non-diabetic NOD mice treated with a-Ab exhibited improved GTT, corresponding to improved GSIS both *in vivo* and *ex vivo* (Figure 1q–s), and a significant increase in islet number and beta-cell mass compared to controls (Figure 1t–v). Alpha cell area was significantly reduced with a-Ab treatment in both NOD and DIO models, suggesting a normalization of islet endocrine populations that may also contribute to improved glycemia (Figure 1w–y, S1m). Collectively, a-Ab-mediated protection against T1D and improvement of glycemic control in a DIO model of T2D are both associated with improved beta-cell mass and function.

Discovery of the FABP4-ADK-NDPK complex (Fabtin)

Despite the influence of hormonal FABP4 on beta-cell mass and function *in vivo* recombinant FABP4 (rFABP4) had no effect on mouse islet GSIS, even at supraphysiological doses (Figure S2a). Previous studies have also been unable to demonstrate a consistent impact of rFABP4 alone on GSIS *in vitro*[16,17]. However, acute rFABP4 administration to WT NOD mice significantly increased blood glucose and reduced plasma insulin compared to vehicle-injected controls at the peak of plasma FABP4 levels (Figure S2b–d). The discordance of *in vitro* and *in vivo* activity suggests that hormonal FABP4 may partner with other proteins to elicit its biological function. This possibility was supported by the structural properties of the FABP4-a-Ab interaction, which exhibits a weak affinity for rFABP4[11]. FABP4 binding by a-Ab is mediated through limited interactions on the light chain (Figure S2e), unlike prototypical antibody-antigen interactions mediated by both the heavy and light chains, or predominantly the heavy chain. Thus, the heavy chain of a-Ab may remain available for additional binding partners. Such a complex would define a novel mechanism of hormone action and shed light into the diverse metabolic functions of hormonal FABP4, including its effects on beta-cells.

To identify potential FABP4 binding partner(s), we performed pulldown and mass spectrometry (MS) using serum from WT glucose intolerant DIO mice[11] and matched DIO FABP4$^{-/-}$ controls. Comparing proteins pulled-down specifically by a-Ab in WT, but not FABP4$^{-/-}$ serum, we identified Adenosine Kinase (ADK) as a top hit (Figure 2a,b). This was intriguing as genetic beta-cell-specific ADK deficiency produces an islet phenotype similar to FABP4-deficiency[18,19]. Pulldowns comparing a-Ab with c-Ab identified another nucleoside kinase, Nucleoside Diphosphate Kinase (NDPK, also known as nm23/nme23/

nme1/nme2) as the top hit (Figure 2a,c). NDPK was bound to a-Ab, but not c-Ab, in both WT and FABP4$^{-/-}$ serum, suggesting a-Ab may independently recognize this protein. To define the a-Ab binding site, we generated nested peptides covering NDPK-A and evaluated interaction with a-Ab by MicroScale Thermophoresis (MST) (Figure S3a). Peptides 2 and 3 had low-affinity binding with a-Ab (μM), while peptide 8 and full-length NDPK-A had comparable high affinity binding (nM) (Figure S3b). No binding was detected between a-Ab and any other peptide, thus the non-overlapping central 5 amino acids of peptide 8 (aa 76–80) is likely the primary epitope for a-Ab (Figure S3c). Examination of the crystal structure for NDPK-A (PDB: 3L7U) places the proposed binding region on the surface, amenable for a-Ab interaction (Figure S3d). Furthermore, the tertiary folding of NDPK-A places peptides 3 and 8 in close-proximity, which may facilitate binding. Together, these findings support the presence of a complex between FABP4-ADK-NDPK *in vivo*, which is targeted by a-Ab through interaction with both FABP4 and NDPK.

MST was also used to validate interactions between the proposed complex components. The strongest interactions were observed between FABP4 and ADK (K_d ~7nM) and ADK and NDPK (K_d ~1.8nM) (Figure 2d; Figure S4a,b). ADK, however, has a relatively weak affinity for a-Ab directly (K_d ~1.9μM; Figure 2d; Figure S4c). We also detected NDPK binding to FABP4 with an affinity of ~700nM (Figure 2d; Figure S4d) and to a-Ab with a K_d of ~150nM (Figure 2d; Figure S4e). Furthermore, using GST-tagged NDPK we were readily able to immunoprecipitate all three components of the proposed complex, as well as the complex with a-Ab (Figure 2e). Interestingly, addition of FABP4 significantly reduced the abundance of ADK bound to GST-NDPK, suggesting FABP4 may act by disrupting the NDPK-ADK interaction (Figure S4f,g). These data provide strong evidence that FABP4 forms a complex with ADK and NDPK, driven by the strong affinities of FABP4 to ADK and ADK to NDPK.

We next explored the function of this complex *in vivo* with an on-bead kinase assay to measure activity of endogenous NDPK and ADK using a-Ab or c-Ab conjugated beads. Both NDPK and ADK are bi-directional kinases that produce ATP or ADP depending on the substrates. Consistent with the MS, ADK activity to generate ATP was specifically observed with a-Ab but not c-Ab (Figure 2f). Furthermore, ADK activity was significantly lower in FABP4$^{-/-}$ serum than WT, supporting that ADK binds to FABP4, and that FABP4 regulate kinase activity in the complex (Figure 2f). To test this, we assessed the ATP and ADP generating activity of recombinant ADK (rADK) with the proposed complex components. FABP4 both alone and in combination with NDPK significantly increased ATP generation by ADK, while NDPK alone had no effect (Figure 2g, Figure S4h). There was no difference in the capacity to generate ADP, suggesting the alteration in activity is uni-directional (Figure S4i).

The on-bead serum pulldown assays also revealed NDPK activity to produce ADP only with a-Ab, but not c-Ab (Figure 2h). Furthermore, we observed increased activity in FABP4$^{-/-}$ serum compared to WT, despite no difference in NDPK abundance, supporting the notion that FABP4 regulates the activity of this complex. Consistent with a high affinity interaction between NDPK and ADK, addition of ADK significantly reduced the ADP-producing activity of NDPK. FABP4 also suppressed NDPK activity, but to a lesser extent, and had

no further effect over addition of ADK, suggesting that ADK is the primary component regulating NDPK activity (Figure 2i; Figure S4j). There was no effect on the capacity of NDPK to produce ATP with addition of FABP4 and/or ADK, suggesting the effect is also uni-directional (Figure S4k).

Addition of a-Ab to either ADK or NDPK alone had no effect on activity (Figure S4l,m), indicating the functional importance of the entire FABP4-ADK-NDPK complex *in vivo.* Addition of a-Ab also had no effect on ADK activity to produce ATP compared to complex alone (Figure 2j). Conversely, a-Ab rescued the ADP-producing capacity of NDPK in the complex, while c-Ab had no effect (Figure 2k). This suggests a-Ab is preventing ADK-mediated suppression of NDPK activity. These observations allowed us to generate a model (Figure 2l) regarding the function of the FABP4-ADK-NDPK complex. Under WT conditions, the FABP4-ADK-NDPK complex has high capacity for ATP production (via ADK) and low ADP production (via NDPK). In the absence of FABP4, ADK activity is reduced, resulting in lower ATP, and inhibition of NDPK is lost, resulting in higher ADP. This relative increase in ADP compared to ATP is phenocopied by targeting the complex using a-Ab.

FABP4-ADK-NDPK impacts GSIS via P2Y1

Unlike rFABP4, which had no effect on GSIS *in vitro* (Figure S2a), addition of NDPK-ADK significantly enhanced GSIS, comparable to the increase observed from FABP4$^{-/-}$ islets (Figure 3a). Further, addition of FABP4 to NDPK-ADK significantly suppressed this response. This was recapitulated in both primary human islets (Figure 3b) and INS1 cells (Figure 3c). Addition of any of the proposed complex components or antibodies alone had no effect (Figure 3b, S5a). In both human islets and INS1 cells, a-Ab rescued FABP4-ADK-NDPK GSIS to levels observed with NDPK-ADK alone, while c-Ab had no effect (Figure 3b,c). This consistent response, in mouse, rat, and human beta-cells supports the conserved relevance of this complex.

At least some functions of intracellular FABP4 have been attributed to its lipid-binding capacity[20]. Importantly, activity of FABP4 to inhibit GSIS was not dependent on lipid binding, as both a lipid binding mutant (LBM) FABP4, and FABP4 treated with the inhibitor BMS-309403, which competes with fatty acid interactions, exhibited the same effect on suppressing NDPK-ADK-potentiated GSIS as WT FABP4 (Figure S5b). Therefore, hormonal FABP4 exhibits a distinct biology, likely independent of its intracellular lipid-binding function as determined by these measures.

Extracellular ATP and ADP signal through cell-surface purinergic G-protein coupled receptors (GPCRs). The predominant receptor on beta-cells is P2Y1, which is potently agonized by ADP and antagonized by ATP, and regulates cAMP, Ca^{2+} fluxes and insulin secretion in both rodents and humans[21,22] (outlined in Figure 3d). Importantly, all substrates required for NDPK and ADK, including ATP, ADP, GTP, and GDP, are released from beta-cells within insulin granules[23]. Endogenous extracellular ATP and ADP regulate GSIS, as made clear upon apyrase treatment, which selectively degrade extracellular ATP (high ratio; producing excess ADP), or ATP and ADP (low ratio; producing excess AMP). Increasing

extracellular ADP while eliminating ATP (high ratio) potently enhanced GSIS from WT mouse islets, while degradation of both ATP and ADP (low ratio) significantly diminished GSIS (Figure 3e). To determine if modulating extracellular nucleoside concentrations could influence complex activity on beta-cell function, we supplemented the complex with ATP or ADP. Addition of exogenous ATP blocked the increase in GSIS by NDPK-ADK to levels observed with FABP4-ADK-NDPK (Figure 3f), consistent with previous findings[24]. This inhibition was more pronounced with ATPγS, a non-metabolizable ATP analog, in-line with metabolism of ATP being part of the complex activity. Conversely, ADP supplementation potentiated GSIS in the presence of the FABP4-ADK-NDPK complex to levels observed with NDPK-ADK alone (Figure 3g).

To elucidate the role of P2Y1 receptors in complex activity, we utilized a potent and selective inhibitor, the nucleotide analog MRS2179[25]. ADP-stimulated GSIS was completely inhibited by MRS2179, confirming inhibitor activity (Figure 3h). Treatment with MRS2179 abolished NDPK-ADK potentiation of GSIS, with no effect in the presence of FABP4-ADK-NDPK, consistent with receptor inhibition by ATP under these conditions (Figure 3i). To confirm that kinase activity of both NDPK and ADK are required to modulate GSIS, we generated a kinase-dead H118N NDPK-A mutant that exhibited no capacity to generate ADP (Figure 3j). Treatment with H118N NDPK and WT ADK had no effect on GSIS, confirming requirement of NDPK kinase activity (Figure 3k). We modeled that GSIS inhibition by the FABP4-ADK-NDPK complex is dependent on the production of ATP by ADK, as activated by FABP4. To test this, we utilized an ADK inhibitor to block the ability of ADK to produce ATP (Figure 3l). Pre-treatment of the complex with the ADK inhibitor improved GSIS equivalent to NDPK-ADK alone, indicating that ATP production by ADK mediates this activity (Figure 3m). Quantification of INS1 supernatant nucleoside abundance also supported this model. NDPK-ADK increased the ADP/ATP ratio, with a corresponding increase in the GTP/GDP ratio, suggesting GDP as the acceptor substrate for an NDPK-dependent reaction (Table S4). Consistently, H118N NDPK with WT ADK failed to alter the ADP/ATP or GTP/GDP ratio. Conversely, addition of ADK inhibitor to the NDPK-ADK-FABP4 complex increased the extracellular ADP/ATP and GTP/GDP ratios, suggesting ADK modulates NDPK activity. Thus, we propose that in the absence of FABP4, or with a-Ab, NDPK increases production of extracellular ADP, resulting purinergic receptor activation and increased GSIS (Figure 3d). When FABP4-ADK-NDPK are in complex, there is a decrease in the extracellular ADP/ATP ratio, which inhibits purinergic receptors, reducing GSIS.

FABP4-ADK-NDPK alters calcium dynamics

P2Y1 activates two downstream signaling pathways, phospholipase C (PLC), which promotes IP_3 generation, and G_i-mediated inhibition of cAMP generation[21,26]. These directly influence Ca^{2+} flux, which regulates both GSIS and survival. Addition of NDPK-ADK reduced pPKA substrate phosphorylation downstream of cAMP, while FABP4-ADK-NDPK enhanced the response (Figure 4a). Further, INS1 cells treated with FABP4-ADK-NDPK exhibit increased phosphorylation of the endoplasmic reticulum (ER) Ca^{2+} efflux transporter IP3R (Figure 4b).

Consistent with reduced GSIS, acute treatment with the FABP4-ADK-NDPK complex significantly decreased glucose-induced extracellular Ca^{2+} influx compared to control or NDPK-ADK (Figure 4c,d). Addition of NDPK-ADK increased Ca^{2+} influx in-line with enhanced GSIS. Activation of IP3R with FABP4-ADK-NDPK treatment suggests there may be increased ER Ca^{2+} efflux into the cytosol. To evaluate this, we performed experiments in the absence of extracellular Ca^{2+}, such that changes in Ca^{2+} could only be sourced from the ER. Upon addition of Thapsigargin (Tg), a sarco/endoplasmic reticulum Ca^{2+} ATPase (SERCA) inhibitor that prevents Ca^{2+} uptake from the cytosol into the ER, ER Ca^{2+} efflux was significantly enhanced in cells with FABP4-ADK-NDPK compared to controls (Figure 4e,f). In both cases, co-treatment with a-Ab was able to rescue Ca^{2+} flux to control levels. Co-treatment with a specific P2Y1 receptor agonist MRS2365 (an ADP mimetic) rescued both Ca^{2+} influx (Figure S6a,b) and ER Ca^{2+} efflux to control levels (Figure S6c,d). The FABP4-ADK-NDPK-induced alteration in ER Ca^{2+} efflux was also rescued by co-treatment with NKY80, an adenylyl cyclase inhibitor which blocks cAMP formation (Figure S6e). Altogether, FABP4-ADK-NDPK signals through P2Y1 to modulate cAMP, resulting in alterations in Ca^{2+} flux and beta-cell dysfunction.

ER Ca^{2+} homeostasis is essential for a variety of processes and reduced ER Ca^{2+} can induce ER stress, impair metabolic processes and compromise survival[27,28]. We observed a significant increase in ER stress marker CHOP with FABP4-ADK-NDPK treatment, as well as increased cleaved caspase 3 (CC3) and pJNK, indicating that chronic exposure to this complex induces beta-cell stress and death (Figure 4g; Figure S6f). In the pathogenesis of diabetes, beta-cells are exposed to numerous stressors including ER dysfunction, lipotoxicity or cytotoxic stress from invading immune cells, which potentiate beta-cell apoptosis. Upon stimulation with FABP4-ADK-NDPK and ER stress-inducer Tg, there was a significant increase in Chop and Bip (Grp78), which were rescued to control levels with a-Ab (Figure 4h, S6g). This corresponded to higher CC3/7 activity, and potentiated cell death (Figure S6h). Additionally, incubation with a cytokine cocktail mimicking immune infiltration in T1D resulted in significantly enhanced CC3/7 activity in the presence of the complex compared to cytokines alone (Figure 4i). Thus, the FABP4-ADK-NDPK complex alters ER Ca^{2+} homeostasis, resulting in ER dysfunction, increased sensitivity to environmental stress, and potentiation of beta-cell death *in vitro*. These mechanisms are critical in both T1D and T2D pathogenesis.

Blocking the FABP4-ADK-NDPK complex preserves beta-cell mass

Given our findings that targeting FABP4-ADK-NDPK with a-Ab improves beta-cell stress resistance and functionality *in vitro*, we wanted to confirm that a-Ab treatment reduces beta-cell death *in vivo*. We observed significant increases in islet number and beta-cell mass with a-Ab treatment in both NOD and DIO models (Figure 1h–j, t-v). The conserved phenotype suggests a direct effect on beta-cells, as there is limited immune influence on beta-cell mass in DIO mice. This is supported by the lack of significant impact on the immune cell profile in pancreata of non-diabetic a-Ab-treated NOD mice (Figure S6i–o, Table S5). To first investigate the contribution of proliferation to the increase in beta-cell mass, NOD mice were given BrdU along with a-Ab, c-Ab, or PBS for 5 weeks beginning at 10 weeks of age. There was no significant difference in the number of BrdU+ beta-cells between a-Ab

and c-Ab (Figure 4j,k). In the DIO model, however, three weeks of a-Ab treatment was associated with a small but significant increase in beta-cell proliferation, as assessed by Ki67 (Figure 4l,m). This is likely associated with the pro-proliferative environment of DIO as compared to NOD. Conversely, and consistent with our *in vitro* findings, we observed a profound reduction in CC3+ beta-cells upon a-Ab treatment compared to controls in both the NOD and DIO models (Figure 4n–q). Thus, targeting the FABP4-ADK-NDPK complex with a-Ab preserves beta-cell mass and enhances beta-cell function to protect against diabetes in multiple models.

Discussion

Hormones are traditionally investigated as solitary entities, with a single hormone released to act through a defined receptor. Here we identified a novel mechanism of hormone biology, wherein circulating FABP4 forms a functional complex with two extracellular nucleoside kinases, NDPK and ADK, to mediate its biological activity. This activity is independent of a defined receptor and is instead regulated through metabolite signaling via purinergic receptors to produce downstream effects. This unique mechanism of action allows for FABP4, the only known hormone to be released from adipose tissue upon stimulation of lipolysis, to have a diverse activity profile, coupling energy fluxes with metabolic response, and establishing a novel endocrine axis of metabolic regulation. We suggest that the FABP4-ADK-NDPK complex likely targets other tissues to influence multiple immunometabolic pathologies where FABP4 is dysregulated and/or purinergic receptor activity is relevant. These may include inflammation, insulin resistance, and various cardiac pathophysiologies that are linked to FABP4 and relevant for purinergic signaling[29,30]. For example, FABP4-ADK-NDPK complex likely acts on hepatocytes to regulate glucose production in obesity, an activity previously attributed to a-Ab treatment[11]. We propose the name Fabtin for this new hormone complex formed by circulating FABP4-ADK-NDPK to indicate its unique constitution.

Supplementary Material

Refer to Web version on PubMed Central for supplementary material.

Acknowledgements

Declaration of Interests

References

1. Jensen MD, Caruso M, Heiling V & Miles JM Insulin regulation of lipolysis in nondiabetic and IDDM subjects. Diabetes 38, 1595–1601, doi:10.2337/diab.38.12.1595 (1989). [PubMed: 2573554]

2. Kim JY et al. Increased lipolysis, diminished adipose tissue insulin sensitivity, and impaired beta-cell function relative to adipose tissue insulin sensitivity in obese youth with impaired glucose tolerance. Diabetes 66, 3085–3090, doi:10.2337/db17-0551 (2017). [PubMed: 28887312]

3. Cao H et al. Adipocyte lipid chaperone AP2 is a secreted adipokine regulating hepatic glucose production. Cell Metab 17, 768–778, doi: 10.1016/j.cmet.2013.04.012 (2013). [PubMed: 23663740]

4. Prentice KJ, Saksi J & Hotamisligil GS Adipokine FABP4 integrates energy stores and counterregulatory metabolic responses. J Lipid Res 60, 734–740, doi:10.1194/jlr.S091793 (2019). [PubMed: 30705117]

5. Saksi J et al. Low-expression variant of fatty acid-binding protein 4 favors reduced manifestations of atherosclerotic disease and increased plaque stability. Circ Cardiovasc Genet 7, 588–598, doi:10.1161/CIRCGENETICS.113.000499 (2014). [PubMed: 25122052]

6. Tuncman G et al. A genetic variant at the fatty acid-binding protein aP2 locus reduces the risk for hypertriglyceridemia, type 2 diabetes, and cardiovascular disease. Proc Natl Acad Sci U S A 103, 6970–6975, doi:10.1073/pnas.0602178103 (2006). [PubMed: 16641093]

7. Zhao W et al. Identification of new susceptibility loci for type 2 diabetes and shared etiological pathways with coronary heart disease. Nat Genet 49, 1450–1457, doi:10.1038/ng.3943 (2017). [PubMed: 28869590]

8. Ertunc ME et al. Secretion of fatty acid binding protein aP2 from adipocytes through a nonclassical pathway in response to adipocyte lipase activity. J Lipid Res 56, 423–434, doi:10.1194/jlr.M055798 (2015). [PubMed: 25535287]

9. Schlottmann I, Ehrhart-Bornstein M, Wabitsch M, Bornstein SR & Lamounier-Zepter V Calcium-dependent release of adipocyte fatty acid binding protein from human adipocytes. Int J Obes (Lond) 38, 1221–1227, doi:10.1038/ijo.2013.241 (2014). [PubMed: 24352293]

10. Villeneuve J et al. Unconventional secretion of FABP4 by endosomes and secretory lysosomes. J Cell Biol 217, 649–665, doi:10.1083/jcb.201705047 (2018). [PubMed: 29212659]

11. Burak MF et al. Development of a therapeutic monoclonal antibody that targets secreted fatty acid-binding protein aP2 to treat type 2 diabetes. Sci Transl Med 7, 319ra205, doi:10.1126/scitranslmed.aac6336 (2015).

12. Thumer L et al. German new onset diabetes in the young incident cohort study: DiMelli study design and first-year results. Rev Diabet Stud 7, 202–208, doi:10.1900/RDS.2010.7.202 (2010). [PubMed: 21409312]

13. Warncke K et al. Does diabetes appear in distinct phenotypes in young people? Results of the diabetes mellitus incidence Cohort Registry (DiMelli). PLoS One 8, e74339, doi:10.1371/journal.pone.0074339 (2013). [PubMed: 24023937]

14. Ziegler AG, Hummel M, Schenker M & Bonifacio E Autoantibody appearance and risk for development of childhood diabetes in offspring of parents with type 1 diabetes: the 2-year analysis of the German BABYDIAB Study. Diabetes 48, 460–468, doi:10.2337/diabetes.48.3.460 (1999). [PubMed: 10078544]

15. Xiao Y et al. Fatty acid binding protein 4 promotes autoimmune diabetes by recruitment and activation of pancreatic islet macrophages. JCI Insight 6, e141814, doi: 10.1172/jci.insight.141814 (2021).

16. Kralisch S et al. Circulating adipocyte fatty acid-binding protein induces insulin resistance in mice in vivo. Obesity (Silver Spring) 23, 1007–1013, doi:10.1002/oby.21057 (2015). [PubMed: 25865078]

17. Wu LE et al. Identification of fatty acid binding protein 4 as an adipokine that regulates insulin secretion during obesity. Mol Metab 3, 465–473, doi:10.1016/j.molmet.2014.02.005 (2014). [PubMed: 24944906]

18. Annes JP et al. Adenosine kinase inhibition selectively promotes rodent and porcine islet beta-cell replication. Proc Natl Acad Sci USA 109, 3915–3920, doi:10.1073/pnas.1201149109 (2012). [PubMed: 22345561]

19. Navarro G et al. Genetic disruption of adenosine kinase in mouse pancreatic beta-cells protects against high-fat diet-induced glucose intolerance. Diabetes 66, 1928–1938, doi:10.2337/db16-0816 (2017). [PubMed: 28468960]

20. Furuhashi M et al. Treatment of diabetes and atherosclerosis by inhibiting fatty-acid-binding protein aP2. Nature 447, 959–965, doi:10.1038/nature05844 (2007). [PubMed: 17554340]

21. Khan S et al. Autocrine activation of P2Y1 receptors couples Ca (2+) influx to Ca (2+) release in human pancreatic beta-cells. Diabetologia 57, 2535–2545, doi:10.1007/s00125-014-3368-8 (2014). [PubMed: 25208758]

22. Leon C et al. The P2Y1 receptor is an ADP receptor antagonized by ATP and expressed in platelets and megakaryoblastic cells. FEBS Lett 403, 26–30, doi:10.1016/s0014-5793(97)00022-7 (1997). [PubMed: 9038354]

23. Detimary P, Jonas JC, & Henquin JC Stable and diffusible pools of nucleotides in pancreatic islet cells. Endocrinology 137, 4671–4676, doi: 10.1210/en.137.11.4671 (1996). [PubMed: 8895332]

24. Bauer C et al. ATP mediates a negative autocrine signal on stimulus-secretion coupling in mouse pancreatic beta-cells. Endocrine 63, 270–283, doi:10.1007/s12020-018-1731-0 (2019). [PubMed: 30229397]

25. Baurand A et al. Inhibition of platelet function by administration of MRS2179, a P2Y1 receptor antagonist. Eur J Pharmacol 412, 213–221, doi:10.1016/s0014-2999(01)00733-6 (2001). [PubMed: 11166284]

26. Seo JB, Jung SR, Hille B & Koh DS Extracellular ATP protects pancreatic duct epithelial cells from alcohol-induced damage through P2Y1 receptor-cAMP signal pathway. Cell Biol Toxicol 32, 229–247, doi:10.1007/s10565-016-9331-3 (2016). [PubMed: 27197531]

27. Engin F et al. Restoration of the unfolded protein response in pancreatic beta-cells protects mice against type 1 diabetes. Sci Transl Med 5, 211ra156, doi:10.1126/scitranslmed.3006534 (2013).

28. Engin F, Nguyen T, Yermalovich A & Hotamisligil GS Aberrant islet unfolded protein response in type 2 diabetes. Sci Rep 4, 4054, doi:10.1038/srep04054 (2014). [PubMed: 24514745]

29. Burnstock G, Vaughn B & Robson SC Purinergic signalling in the liver in health and disease. Purinergic Signal 10, 51–70, doi:10.1007/s11302-013-9398-8 (2014). [PubMed: 24271096]

30. Burnstock G Purinergic signaling in the cardiovascular system. Circ Res 120, 207–228, doi:10.1161/CIRCRESAHA.116.309726 (2017). [PubMed: 28057794]
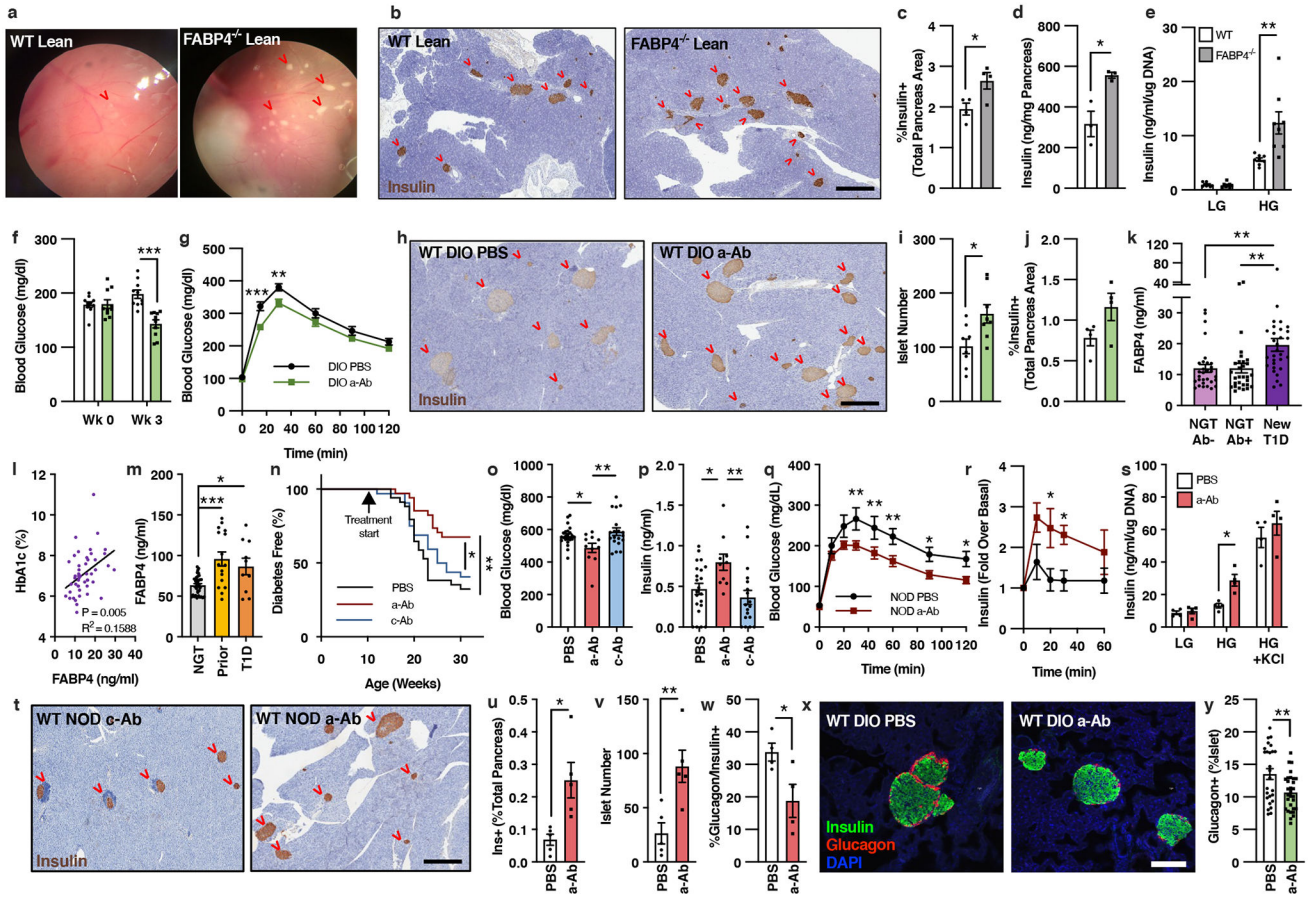
Figure 1. Depletion of FABP4 increases beta-cell mass and function

(a) Gross pancreas images in lean wild type (WT) and FABP4$^{-/-}$ mice. (b) Insulin immunohistochemistry (IHC) in pancreatic sections from 7-wk-old WT or FABP4$^{-/-}$ mice (N=4/group). (c) Quantification of percentage insulin positive area per total pancreatic area based on IHC (N=4/group; P=0.0318). (d) Total pancreatic insulin content from 7-wk-old WT and FABP4$^{-/-}$ mice (N=3/group; P=0.0198). (e) Glucose-stimulated insulin secretion (GSIS) from islets *ex vivo* under low glucose (2.8mM; LG) and high glucose (16.7mM; HG) conditions (N=8/group; P=0.006008). (f) 6hr fasting blood glucose from diet-induced obese (DIO) mice before treatment (wk 0) and following a-Ab for 3 wks (N=10/group; P=0.000064). (g) Glucose tolerance test (GTT) in DIO mice treated for 2 wks with PBS or a-Ab (N=10/group). (h) Insulin IHC in pancreatic sections from DIO mice treated with PBS or a-Ab for 3 wks (N=6/group) with (i) quantification of total islet number per pancreatic section (N=8/group; P=0.0157), and (j) percentage of insulin positive area per total pancreatic area (N=4/group). (k) Plasma FABP4 levels in autoantibody positive and negative normal glucose tolerant (NGT) individuals compared to new-onset T1D patients (<1-year duration; BABYDIAB and DiMELLI cohorts) (N=30/group; Ab+ vs. T1D P=0.0049; Ab- vs. T1D P=0.0047). (l) Correlation of plasma FABP4 with HbA1c percentage in established T1D patients (BRI cohort; N=50/group). (m) Plasma FABP4 levels in NOD mice while NGT, one week prior to hyperglycemia (Prior), or at time of T1D onset (N=35 (NGT), 16 (Prior), 10 (T1D); NGT vs. Prior P<0.00001; NGT vs. T1D

P=0.0193). (n) Incidence curve for NOD model of T1D following treatment with PBS, a-Ab, or c-Ab beginning at 10 wks of age (N=36/group; P=0.0079). (o) Average blood glucose of NOD mice at the time of T1D diagnosis (N=23 (PBS), 11 (a-Ab), 19 (c-Ab); PBS vs. a-Ab P=0.0491; a-Ab vs. c-Ab P=0.0072). (p) Plasma insulin levels prior to T1D diagnosis in NOD mice (N=22 (PBS), 10 (a-Ab), 18 (c-Ab); PBS vs. a-Ab P=0.0350; a-Ab vs. c-Ab P=0.0055). (q) GTT and (r) corresponding plasma insulin values in non-diabetic NOD mice treated with PBS or a-Ab (N=6/group). (s) GSIS from islets isolated from NOD mice treated with PBS or a-Ab for 15 wks (N=4/group; P=0.0452). (t) Insulin IHC and quantification of (u) percentage of insulin positive area per total pancreatic area (P=0.0125), and (v) islet number per pancreatic section from mice treated with a-Ab or c-Ab for 5 wks (N=5/group; P=0.0085). (w) Quantification of insulin and glucagon immunofluorescence (IF) in pancreatic sections of NOD mice treated with a-Ab or c-Ab for 5 wks (N=4/group; P=0.0409). (x) IF and (y) quantification of insulin (green) and glucagon (red) staining in pancreatic sections of DIO mice treated with a-Ab or PBS for 3 wks (N=26 (PBS) and 30 (a-Ab) islets from 5 mice/group; P=0.0044). Scale bars for panels 500um (b,h,t) and 200um (x). *P<0.05, **P<0.01, ***P<0.001. Data are mean +/− SEM. Two-tailed unpaired *t*-test (c-f,I,j,u,v,w,y); One-way ANOVA (k,m,o,p); Two-way ANOVA (g,q,r,s); Simple linear regression correlation (l); Log-rank Mantel-Cox test (n).
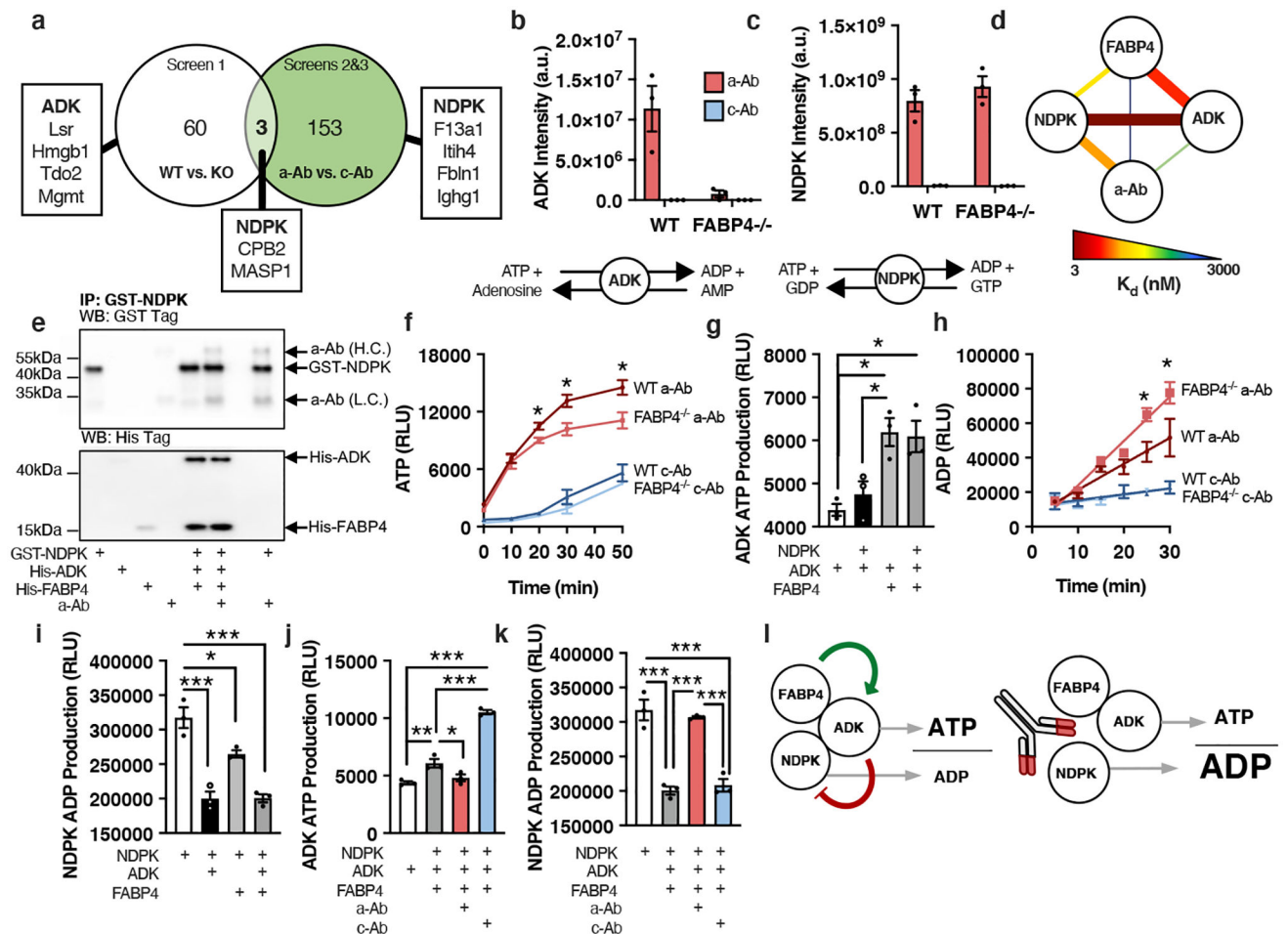
Figure 2. Circulating FABP4 forms a hormonal complex with NDPK and ADK to regulate extracellular nucleosides.

(a) Results of three independent immune-precipitation (IP) and mass spectrometry experiments from WT or FABP4$^{-/-}$ DIO serum with a-Ab or c-Ab with top hits based on enrichment and spectral counts. Spectral counts of (b) ADK and (c) NDPK from Screen 1 (N=3/group). (d) Summary of MST among proposed complex components (N=6/interaction). (e) IP of GST-tagged NDPK with each of the proposed complex components and a-Ab (LC, light chain; HC, heavy chain; N=4). (f) On-bead ADK kinase assay for ATP production from WT or FABP4$^{-/-}$ mouse serum (N=5/group). (g) ATP production from recombinant ADK in the presence of complex components (N=3/group; ADK vs. ADK FABP4 P=0.0113; ADK vs FABP4-ADK-NDPK P=0.0154; ADK-NDPK vs. ADK FABP4 P=0.0360). (h) On-bead NDPK kinase assay for ADP production from WT or FABP4$^{-/-}$ mouse serum (N=5/group). (i) ADP production from recombinant NDPK in the presence of complex components (N=3/group; NDPK vs. NDPK ADK P=0.0001; NDPK vs. NDPK FABP4 P=0.0221; NDPK vs. FABP4-ADK-NDPK P=0.0001). (j) ADK activity to produce ATP in the presence of complex components with a-Ab or c-Ab (N=3/group; ADK vs. FABP4-ADK-NDPK P=0.0076; FABP4-ADK-NDPK vs. a-Ab P=0.0340; ADK vs. c-Ab P<0.0001; FABP4-ADK-NDPK vs. c-Ab P<0.0001; a-Ab vs. c-Ab P<0.0001). (k) NDPK activity to produce ADP in the presence of complex components with a-Ab or
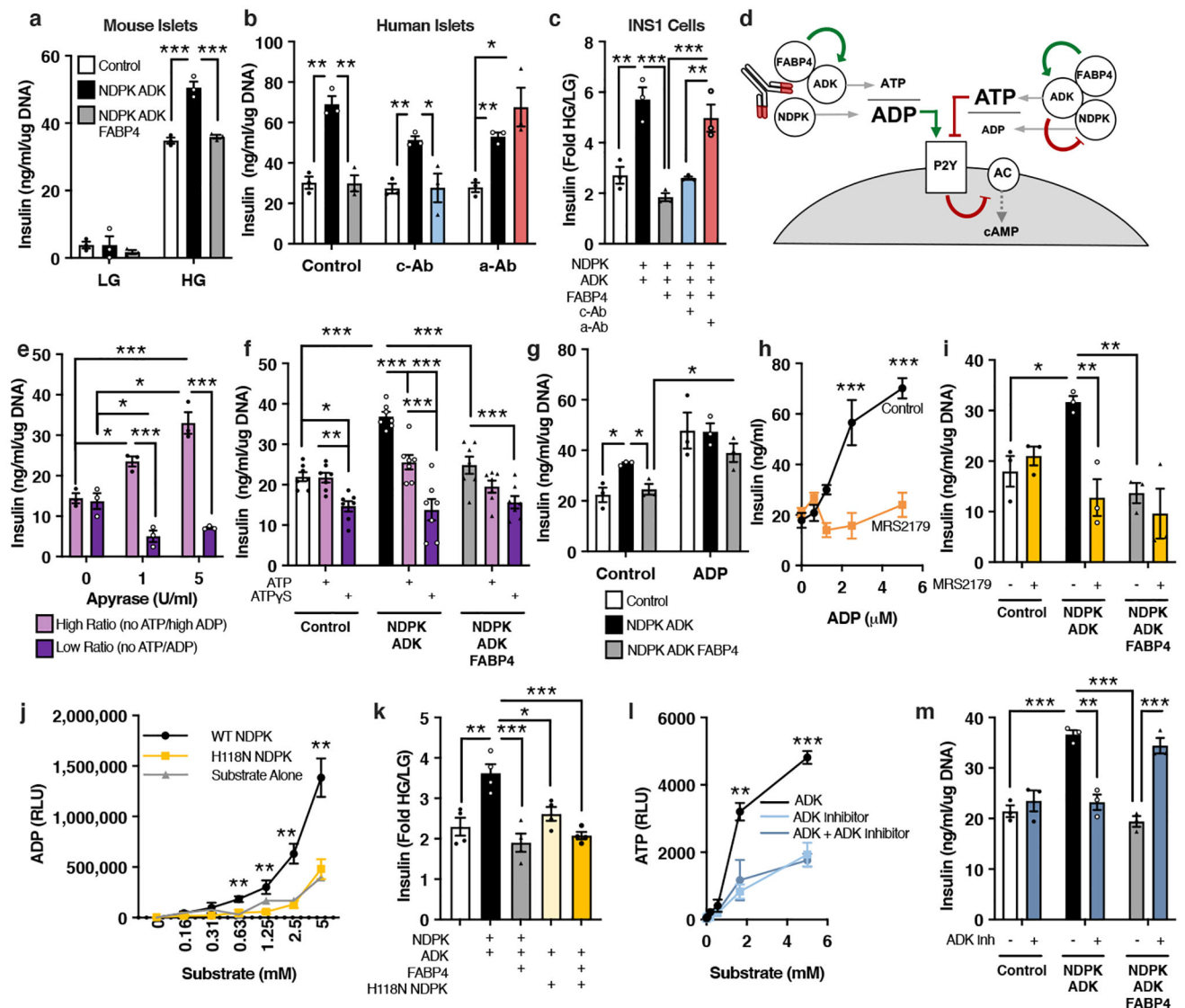
c-Ab (N=3/group; NDPK vs. FABP4-ADK-NDPK P<0.0001; NDPK vs. c-Ab P=0.0002; FABP4-ADK-NDPK vs. a-Ab P=0.0002; a-Ab vs. c-Ab P=0.0003). (l) Proposed model of extracellular nucleoside regulation from the complex. *P<0.05, **P<0.01, ***P<0.001. Data are mean +/− SEM. Two-way ANOVA (f,h); One-way ANOVA (g,i-k).

Figure 3. The FABP4-ADK-NDPK complex inhibits GSIS and is neutralized by a-Ab.
GSIS from (a) WT primary mouse islets (N=3/group; P<0.0001), (b) human islets (N=3/
group; Control vs. NDPK-ADK P=0.0038; NDPK-ADK vs. FABP4-ADK-NDPK P=0.0049;
Control c-Ab vs. NDPK-ADK c-Ab P=0.0043; NDPK-ADK c-Ab vs. FABP4-ADK-NDPK
c-Ab P=0.0230; Control a-Ab vs. NDPK-ADK a-Ab 0.0031; NDPK-ADK a-Ab vs.
FABP4-ADK-NDPK a-Ab P=0.0067) and (c) INS1 cells with complex components (N=3/
group; Control vs. NDPK-ADK P=0.0012; NDPK-ADK vs. FABP4-ADK-NDPK P=0.0002;
FABP4-ADK-NDPK vs. a-Ab P=0.0009; c-Ab vs. a-Ab P=0.0066). (d) Proposed model
for the activity of FABP4-ADK-NDPK on P2Y1. (e) GSIS from WT mouse islets treated
with high ratio (ATP degrading) or low ratio (ATP and ADP degrading) apyrase (N=3/
group). GSIS from INS1 cells treated with control, NDPK-ADK, or FABP4-ADK-NDPK
in the presence of (f) 5uM ATP or non-metabolizable ATPγS (N=7/group) and (g) 5uM
of ADP (N=3/group; Control vs. NDPK-ADK P=0.0132; NDPK-ADK vs. FABP4-ADK-
NDPK P=0.0307; FABP4-ADK-NDPK vs. FABP4-ADK-NDPK ADP P=0.0273). (h) GSIS

from INS1 cells with ADP in the presence or absence of P2Y1 antagonist MRS2179 (N=4/group). (i) GSIS from INS1 cells treated with NDPK-ADK or FABP4-ADK-NDPK in the presence of MRS2179 (N=3/group; Control vs. NDPK-ADK P=0.0232; NDPK-ADK vs. FABP4-ADK-NDPK P=0.0038; NDPK-ADK vs. NDPK-ADK MRS2179 P=0.0026). (j) Kinase activity of WT NDPK or kinase dead H118N NDPK to produce ADP (N=4/group). (k) GSIS from INS1 cells treated with WT NDPK or H118N NDPK in combination with ADK and FABP4 (N=4/group). (l) Kinase activity of ADK to generate ATP in the presence of ADK inhibitor (N=4/group). (m) GSIS from INS1 cells treated with NDPK-ADK or FABP4-ADK-NDPK in the presence of ADK inhibitor (N=3). In all cases, low glucose (LG; 2.8mM), high glucose (HG; 16.7mM). *P<0.05, **P<0.01, ***P<0.001. Data are mean +/− SEM. Two-way ANOVA (a,b,e-m); One-way ANOVA (c).
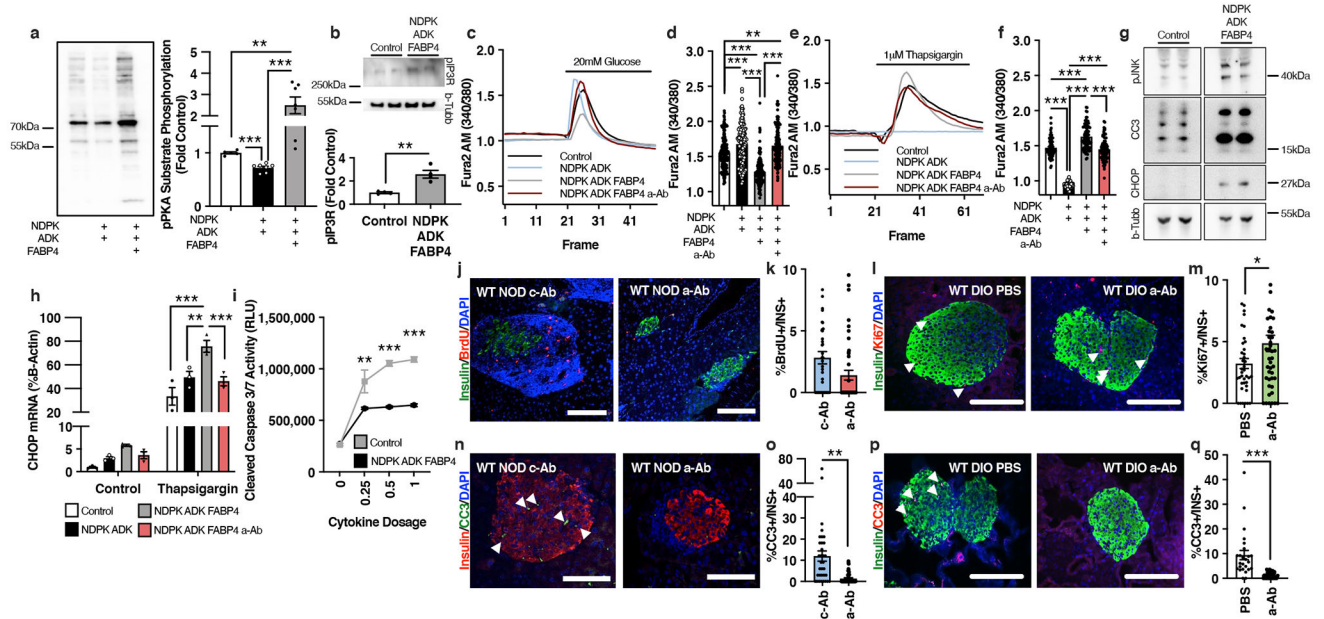
Figure 4. The FABP4-ADK-NDPK complex alters beta-cell calcium dynamics and promotes cell death.

(a) Western blot (WB) and quantification of pPKA substrate phosphorylation in human islets treated with NDPK-ADK or FABP4-ADK-NDPK (N=6; Control vs. NDPK-ADK P<0.0001; NDPK-ADK vs. FABP4-ADK-NDPK P=0.0007; Control vs. FABP4-ADK-NDPK P=0.0095). (b) WB and quantification of pIP3R in INS1 cells treated with FABP4-ADK-NDPK (N=4; P=0.0034). Cytosolic calcium flux in INS1 cells from (c,d) the extracellular space in response to glucose (N=3 coverslips, 150 cells/condition except NDPK-ADK 144 cells) and (e,f) the ER in response to 1uM thapsigargin by Fura-2 AM staining (N=3 coverslips, 75 cells/condition except NDPK-ADK 100 cells). (g) WB for cleaved caspase 3 (CC3), pJNK, Chop, and B-Tubulin from INS1 cells treated with FABP4-ADK-NDPK for 24hrs (N=4). (h) Gene expression of ER stress marker Chop following 2hr treatment with complex components in the presence or absence of Tg (N=3; Control vs. FABP4-ADK-NDPK P<0.0001; NDPK-ADK vs. FABP4-ADK-NDPK P=0.0012; FABP4-ADK-NDPK vs. a-Ab P=0.0003). (i) Cleaved caspase 3/7 activity in INS1 cells treated with cytokine cocktail (TNFa, IFNg and IL-1b) with or without FABP4-ADK-NDPK (N=4/group). (j) IF for insulin (green), BrdU (red), and nuclei (DAPI; blue) and (k) quantification of pancreatic sections from NOD mice treated with BrdU and a-Ab or c-Ab for 5wks (N=5 mice/group; 48 (c-Ab), 46 (a-Ab) islets). (l) IF for insulin (green), Ki67 (red), and nuclei (DAPI; blue) and (m) quantification of pancreatic sections from DIO mice treated with PBS or a-Ab for 3 weeks (N=5 mice/group; 39 (PBS), 45 (a-Ab) islets; P=0.0437). (n) IF staining of pancreatic sections from NOD mice treated with a-Ab or c-Ab for insulin (red), CC3 (green) and nuclei (DAPI; blue) with (o) quantification of CC3 and insulin co-stained cells (N=5 mice/group; 33 (c-Ab), 45 (a-Ab) islets; P=0.0010). (p) IF of pancreatic sections from DIO mice treated with PBS or a-Ab for insulin (green), CC3 (red) and nuclei (DAPI; blue) with (q) quantification of CC3 and insulin co-stained cells (N= 5 mice/group; 25 (PBS), 34 (a-Ab) islets; P<0.0001). Scale bars are 150um (j,l,p) and 100um (n). *P<0.05, **P<0.01,

***P<0.001. Data are mean +/− SEM. One-way ANOVA (d,f); Two-tailed unpaired *t*-test (a,b,k,m,o,q); Two-way ANOVA (h,i).